

Bootstrap methods for estimating spatial synchrony of fluctuating populations

Magnar Lillegård, Steinar Engen and Bernt-Erik Sæther

Lillegård, M., Engen, S. and Sæther, B.-E. 2005. Bootstrap methods for estimating spatial synchrony of fluctuating populations. – *Oikos* 109: 342–350.

We describe and examine methods for estimating spatial correlations used in population ecology. We base our analyses on a hypothetical example of a species that has been censused at 30 different locations for 20 years. We assume that the population fluctuations can be described by a simple linear model on logarithmic scale. Stochastic simulations is utilized to check how seven different ways of resampling perform when the goal is to find nominal 95% confidence intervals for the spatial correlation in growth rates at given distances. It turns out that resampling of locations performs badly, with true coverage level as low as 30–40%, especially for small correlations at long distances. Resampling of timepoints performs much better, with coverage varying from 80 to 90%, depending on the strength of density regulation and whether the spatial correlation is estimated for the response variable or for the error terms in the model. Assuming that the underlying model is known, the best results are achieved for parametric bootstrapping, a result that strongly emphasize the importance of defining and estimating a proper population model when studying spatial processes.

M. Lillegård and S. Engen, Dept of Mathematical Sciences, Norwegian Univ. of Science and Technology, NO-7491 Trondheim, Norway (magnarl@math.ntnu.no). – B.-E. Sæther, Dept of Biology, Norwegian Univ. of Science and Technology, NO-7491 Trondheim, Norway.

Synchronous fluctuations in size of populations that are geographically separated from each other have now been demonstrated in many taxa, including birds (Ranta et al. 1995, Cattadori et al. 1999, 2000, Paradis et al. 1999, 2000), fishes (Myers et al. 1997), insects (Hanski and Woiwood 1993, Sutcliffe et al. 1996, Myers 1998) and mammals (Moran 1953, Royama 1992, Ranta et al. 1997, Haydon et al. 2001). A general pattern that emerges is large interspecific variation in the scaling of the synchrony in the population fluctuations, even among closely related species (Lindström et al. 1996, Paradis et al. 2000, Williams et al. 2003). Theoretical analyses have suggested that the scaling should increase with dispersal distance and spatial environmental auto-correlation, but decrease with the strength of density regulation (Moran 1953, Ranta et al. 1997, 1998, Lande et al. 1999, 2003:79–100, Bjørnstad and Bolker 2000,

Kendall et al. 2000, Engen 2001, Engen et al. 2002a, b, Peltonen et al. 2002). Disentangling the relative contribution of these processes to variation in spatial scaling in population fluctuations have however been difficult (Bjørnstad et al. 1999b).

One reason for the lack of mechanistic understanding of the process generating spatial patterns in population fluctuations may be that many of the statistical methods are developed in fields where the access to data is large, like in many geostatistical applications (Chilès and Delfiner 1999) or in image analysis (Winkler 1995). In ecology temporal fluctuations in population size are an additional major component of interest that must be included together with spatial properties. Many of the available time series are however in a statistical sense short (Lande et al. 2002, 2003:64–68), and applications of spatial statistical methods in ecology will therefore

Accepted 12 November 2004

Copyright © OIKOS 2005
ISSN 0030-1299

often stretch the limits of established statistical methods because the properties of the methods will be partly unknown. One example that illustrates this point is that temporal trends often are removed prior to analyses of ecological time series (Viljugrein et al. 2001). This is based on the explicit assumption that the amount of data is large enough to claim that the mean value, or the mean as a linear function of time, is practically known. It is forgotten that for short time series the mean value only can be estimated with large uncertainty, especially when the temporal autocorrelations and return time to equilibrium are large. This is a major problem in the estimation of the strength of density dependence (Lande et al. 2002) because if there is large uncertainty in the estimate of the carrying capacity, it is difficult to estimate the rate by which the population size will return to this partly unknown value.

Access to spatial replicates of time series is important for several reasons. First, it enables analysis of the spatial properties of population fluctuations (Dennis et al. 1998). Second, even replications that are spatially correlated increase the amount of information that can be derived to characterize the temporal fluctuations in population size. Although a long return time to equilibrium is a problem when estimating density regulation, we shall demonstrate that the opposite is the case when it comes to drawing inference on the spatial scaling of population fluctuations. This is due to the fact that the yearly realized growth rates are less correlated when density regulation is weak and hence gives a larger amount of information.

The present paper deals with statistical inference of spatial scaling of population fluctuations. We first review different definitions and measurements of such spatial scaling. Then we examine different ways of estimating spatial correlations used in population ecology, and, finally, we choose a simple linear model on the log scale to check through stochastic simulations how seven different ways of bootstrapping perform when the goal is to find confidence intervals or uncertainties in parameters defining the spatial scaling of population fluctuations.

Measurements of spatial synchrony

Spatial autocorrelations may be measured in several different ways. First, measurements can be defined directly for the population size or for the log of population size. In theoretical models based on linearizations on the absolute scale, it is natural also to define spatial scaling on this scale (Lande et al. 1999, Engen et al. 2002a). However, it is often more realistic to assume that models are linear on the log scale, and in this case measurements of scaling are most conveniently

defined using the log scale (Engen 2001, Engen et al. 2002b).

Second, the scaling may be defined for the actual (log) population sizes, for the between years differences in these, or for the residuals obtained after fitting a stochastic model subtracting the estimated mean change in (log) population size. Engen et al. (2002a) have analyzed theoretically how spatial scaling for these different quantities are affected by the strength of local density regulation, spatial autocorrelation in the environmental noise, and the migration of individuals.

Regardless the choice of scale or choice of variable for defining spatial correlation, the spatial correlation for two measurements made simultaneously with spatial distance z can conveniently be written on the form

$$\rho(z) = (\rho_0 - \rho_\infty)h(z) + \rho_\infty \quad (1)$$

for $z \neq 0$ and $\rho(0) = 1$. In our analysis of bootstrap methods we use the exponential model $h(z) = e^{-z/l}$. The function ρ (Fig. 1) is the so-called correlogram (Cressie 1993:67) and has wide applications in population ecology (Bjørnstad et al. 1999a, b, Koenig 1999, 2002). The variable z may be two-dimensional, expressing the spatial distance and the direction between two points in the plane. Usually one deals with isotropic models so that z can be defined as the euclidean distance. Here $h(0) = 1$, $h(\infty) = 0$ and $h(z)$ has to be defined in a way so that the function ρ is positive definite (Johnson and Wichern 1988:48) and $|\rho(z)| \leq 1$. If ρ_0 is smaller than 1 we have a so-called nugget effect (Matheron 1962), expressing that the correlation decreases discontinuously at zero. This is often realistic due to demographic stochasticity and sampling errors. The parameter ρ_∞ expresses long distance correlations that may be generated either by an environmental noise component

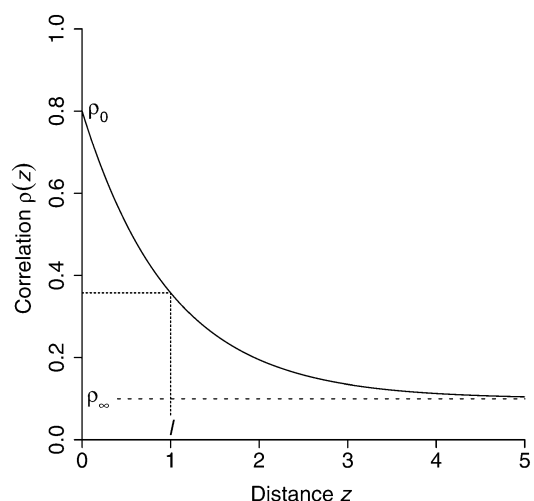


Fig. 1. Structure of the spatial correlation function ρ (the correlogram). The parameters ρ_0 and ρ_∞ denote the correlations at zero and infinite distance, respectively, whereas l represents the scaling. We have $\rho_0 = 0.8$, $\rho_\infty = 0.1$ and $l = 1$.

common for all local sites, or long distance migration (Lande et al. 2003).

Measures of spatial scaling, say l , are always defined by properties of the function $h(z)$. Roughgarden (1975) used the distance l at which $h(l) = e^{-1}$. If $h(z)$ is an exponential function, this measure is exactly the same as the standard deviation of the distribution obtained by scaling $h(z)$ to become a distribution. The standard deviation of this distribution may generally be used as a measurement of spatial scaling when $h(z) \geq 0$. Applying this measure, Lande et al. (1999), Engen (2001) and Engen et al. (2002a, b) found a number of results relating the spatial scaling to density regulation, migration and spatially autocorrelated noise.

The model

Write $N_{i0}, N_{i1}, \dots, N_{iT}$ for the time series giving the number of individuals from time zero to T at location i , $i = 1, \dots, n$. Using a theta-logistic type of density regulation with $\theta = 0$ (Lande et al. 2003:110), the mean and variance of changes in N takes the form $E(\Delta N|N) = rN(1 - \ln N/\ln K)$ and $\text{var}(\Delta N|N) = \sigma^2 N^2$, where K is the carrying capacity and σ^2 is the environmental variance.

We focus on the changes in $\ln N$, the population growth rate, where the mean and variance are approximately

$$E(\Delta \ln N|\ln N) = \alpha - \beta \ln N \quad (2)$$

$$\text{var}(\Delta \ln N|\ln N) = \sigma^2 \quad (3)$$

where $\alpha = r - \sigma^2/2$ and $\beta = r/\ln K$.

Write $D = \Delta \ln N$ for convenience. In discrete time, the model for the times series of growth rates at location i is given by

$$D_{it} = \ln N_{it} - \ln N_{i,t-1} = \alpha - \beta \ln N_{i,t-1} + W_{it} \quad (4)$$

for $t = 1, \dots, T$, where the error terms W_{i1}, \dots, W_{iT} are independent normally distributed with mean zero and variance σ^2 . This is a linear model frequently used in time series of population fluctuations (Royama 1992). A β -value close to zero indicates a weak density regulation in the population, whereas a β -value close to one indicates a strong density regulation. The stationary distribution of $\ln N$ is the normal distribution with mean α/β and variance $\sigma^2/\{1 - (1 - \beta)^2\}$.

The error terms $W_{1t}, W_{2t}, \dots, W_{nt}$ for locations $1, 2, \dots, n$ at time t are exogenous factors, e.g. weather, that can have the same influence on many populations. This influence produces a spatial correlation between the populations. According to Moran (1953) populations with common linear autoregressive models will have the same correlation as the shared exogenous factors, i.e. (D_{1t}, \dots, D_{nt}) has the same correlation matrix as (W_{1t}, \dots, W_{nt}) . The correlations are given by Eq. (1).

Methods

Estimation of spatial correlation

Write the observations by the matrix

$$\begin{matrix} D_{11} & D_{12} & \cdots & D_{1T} \\ D_{21} & D_{22} & \cdots & D_{2T} \\ \vdots & \vdots & \cdots & \vdots \\ D_{n1} & D_{n2} & \cdots & D_{nT} \end{matrix} \quad (5)$$

where row i is the time series for location i , and column t is the observations at time t .

The correlation between locations i and j is estimated using the standard formula for independent observations from a bivariate distribution

$$\hat{\rho}(z) = \frac{\sum_{t=1}^T (D_{it} - \bar{D}_i)(D_{jt} - \bar{D}_j)}{\sqrt{\sum_{t=1}^T (D_{it} - \bar{D}_i)^2 \sum_{t=1}^T (D_{jt} - \bar{D}_j)^2}}$$

If there is no density regulation, that is, $\beta = 0$, the processes are random walks, and the growth rates D_{i1}, \dots, D_{iT} are independent. Then the pairs $(D_{i1}, D_{j1}), \dots, (D_{iT}, D_{jT})$ are independent observations from a bivariate normal distribution with correlation $\rho(z)$. In this case the properties of the correlation estimates $\hat{\rho}(z)$ are well known. For example, one may use the arctanh transformation $\hat{w} = 0.5 \ln\{(1 + \hat{\rho})/(1 - \hat{\rho})\}$ which is an approximately unbiased estimator for $0.5 \ln\{(1 + \rho)/(1 - \rho)\}$ and has approximate variance $1/(T - 3)$ (Fisher 1915, 1921). All the unknown parameters in the model can be estimated simultaneously by maximum likelihood methods using the fact that we have T independent observations from a multinormal distribution.

For density regulated populations, however, the pairs $(D_{i1}, D_{j1}), \dots, (D_{iT}, D_{jT})$ are not independent (Appendix), hence Fisher's results are not applicable. A usual approach, which is common for all the methods in this paper, is to plot the $n(n - 1)/2$ possible points of distance and estimated correlation, $(z, \hat{\rho}(z))$ say, in a scatter diagram and estimate the correlogram ρ through simple regression techniques, for example least squares, or non-parametric approaches like the spline method (Bjørnstad and Falck 2001). The uncertainty of the estimated correlogram is then found by bootstrapping.

The problem of estimating spatial correlation when we have only one observation at each location is discussed in Appendix 1.

Bootstrapping

The assumption of independence between data is crucial to the success of bootstrapping (Efron and Tibshirani 1993:45–56 for details about bootstrapping). Space-time data are generally not independent, thus a straightforward application of the bootstrap method to find the

uncertainty of the estimated correlogram is not appropriate (Cressie 1993:100). Good approaches have been suggested on spatial, but not temporal, data (Lahiri et al. 1999, Zhu and Morgan 2004), but bootstrapping methods used on space-time data may fail dramatically. Here we examine some existing methods and propose simple alternatives. These are all methods that generate bootstrap replications of the scatter diagram of distance and correlation points, and, from this, bootstrap replications of the estimated correlogram. Table 1 gives a short summary of the different methods used in the analyses. All the methods are used on a hypothetical example consisting of 30 locations censured for 20 years.

Given bootstrap replications of the estimated correlogram, its uncertainty can be approximated by bootstrap confidence intervals. Such an interval is calculated from the ordered sample of B bootstrap replications of $\hat{\rho}(z)$, $\hat{\rho}_{(1)}^*, \dots, \hat{\rho}_{(B)}^*$, say, for a given distance z . Provided that $B\alpha/2$ is an integer, a nominal $100(1-\alpha)\%$ bootstrap confidence interval for $\rho(z)$ is given by

$$[\hat{\rho}_{(B\alpha/2)}^*, \hat{\rho}_{(B(1-\alpha/2))}^*] \quad (6)$$

The phrase “nominal $100(1-\alpha)\%$ ” means that the interval is supposed to cover $\rho(z)$ with confidence $100(1-\alpha)\%$, but this may not reflect the true confidence level (coverage) of the interval. The coverage can be estimated through simulation studies, that is, by computing a large number of intervals for different simulated data sets and finding the relative frequency of intervals that cover $\rho(z)$.

Resampling of locations

Method I

Method I is used by Bjørnstad et al. (1999a, b), Bjørnstad and Falck (2001), Peltonen et al. (2002) and Tobin and Bjørnstad (2003). They make a resample of the locations, which is another way to say that they draw n locations with replacement from $1, 2, \dots, n$. Then they calculate all points of distance and correlation based on the locations in this resample and discard the calculations which give distance zero and correlation one due to sampling of one location more than once. For example,

Table 1. Summary of the bootstrap methods.

Method	Description	Variable used
I	resampling of locations	growth rates
II	resampling of location pairs	growth rates
III	resampling of columns in the observation matrix	growth rates
IV	resampling of columns in the residual matrix	residuals
V	resampling of columns in the residual matrix	growth rates
VI	parametric bootstrapping	growth rates
VII	parametric bootstrapping	error terms

say we have five locations $1, 2, \dots, 5$. One resample could be $2, 5, 3, 1$ and 1 , giving six points in the bootstrap replication of the scatter diagram, one point for each of the location pairs

$$(1, 2), (1, 3), (1, 5), (2, 3), (2, 5), (3, 5).$$

This is equivalent to sampling a random number of points without replacement from the observed scatter diagram and consequently not what is known as bootstrapping, which should be sampling with replacement.

Method II

A related approach is to draw a resample of pairs from the $n(n-1)/2$ pairs of locations and calculate new points of distance and correlation based on this resample. If we have five locations $1, 2, \dots, 5$, we draw 10 location pairs with replacement from $(1, 2), (1, 3), \dots, (4, 5)$. One such resample could be

$$(1, 5), (3, 4), (1, 3), (1, 3), (2, 3), (2, 3), (2, 3), (1, 3), (1, 3), (1, 5),$$

giving 10 points in the bootstrap replication of the scatter diagram, with some points overlapping. This is equivalent to the resampling of points from the observed scatter diagram.

Method II, as well as method I, has some serious weaknesses. First, when we resample points in the observed scatter diagram we sample from elements which are not independent. They are dependent due to the fact that the same location appears in more than one point. For example, if a location i is highly correlated with both locations j and k , we would expect the locations j and k to be highly correlated as well.

Second, bootstrapping should be carried out in a manner that reflects the original randomness of the data (Buonaccorsi et al. 2001), i.e. the objects that are resampled should be a random sample from some probability distribution. However, locations are usually fixed and hence cannot be regarded as a random sample.

Resampling of timepoints

Method III

Write $D_t = (D_{1t}, D_{2t}, \dots, D_{nt})'$ for the observations at time t , the apostrophe denoting transpose. Hence the observation matrix (5) can be written as $D_1 D_2 \dots D_T$. Draw a resample of the timepoints $1, 2, \dots, T$, and denote the resample t_1, t_2, \dots, t_T . For example, if we have six timepoints $1, 2, \dots, 6$, one resample could be $6, 1, 5, 2, 5$ and 5 , hence $t_1=6, t_2=1, t_3=5, t_4=2, t_5=5$ and $t_6=5$. Replacing the original time points with the resample, we get a resample of observations given by

$$D_{t_1} D_{t_2} \dots D_{t_T}$$

In the example given above, this equals $D_6 D_1 D_5 D_2 D_5 D_5$. In other words, this is a resample of the T columns in

the observation matrix (5). A bootstrap replication of the scatter diagram is now calculated from this resample of observations.

Bootstrapping should be performed from independent observations. The autocorrelation between two observations D_{it} and $D_{i,t+s}$ in a time series equals $-\beta(1-\beta)^s - 1/2$ (Appendix 1 for computational details), hence the serial correlation almost vanishes under weak density regulation, i.e. for small values of β . Under this assumption, this bootstrap method is, according to general theory on bootstrapping (Efron and Tibshirani 1983:45–56), expected to perform well.

Method IV

If there is a serial correlation within each time series, that is, for strong density regulation (large β), resampling of residuals may be a better approach because the error terms W_{it} , $t=1, \dots, T$, are ideally serially independent. This procedure is sometimes called “prewhitening” and is used by Williams and Liebhold (2000) and Buonaccorsi et al. (2001). Writing $\hat{\alpha}$ and $\hat{\beta}$ for the estimates of α and β we calculate the residuals $e_{it} = D_{it} - (\hat{\alpha} - \hat{\beta} \ln N_{i,t-1})$ and write $e_t = (e_{1t}, e_{2t}, \dots, e_{nt})'$. Draw a resample t_1, t_2, \dots, t_T of the timepoints $1, 2, \dots, T$, and let the resample of residuals be

$$e_{t_1} e_{t_2} \dots e_{t_T}$$

which is a resample of the columns in the residual matrix corresponding to (5). Finally we utilize the fact that the error terms W_{it} in our model have the same spatial correlation structure as the D_{it} values, hence a bootstrap replication of the scatter diagram can be calculated from the resampled residuals.

Method V

Estimate the expected growth rate for location i at time t by $\hat{D}_{it} = \hat{\alpha} - \hat{\beta} \ln N_{i,t-1}$, and write $\hat{D}_t = (\hat{D}_{1t}, \hat{D}_{2t}, \dots, \hat{D}_{nt})'$ for the estimated growth rates at time t . Calculate a resample of observations by

$$(\hat{D}_1 + e_{t_1})(\hat{D}_2 + e_{t_2}) \dots (\hat{D}_T + e_{t_T})$$

where $e_{t_1}, e_{t_2}, \dots, e_{t_T}$ is the resample of residuals given in method IV. Notice that this method is similar to the method of bootstrapping residuals in a regression model (Efron and Tibshirani 1983:113).

By resampling timepoints, the correlations in the bootstrap replication of the scatter diagram will be different from the observed correlations. Hence methods III, IV and V are not based on sampling from the observed scatter diagram, and the dependence between the points in the diagram should no longer be a problem.

Parametric bootstrapping

Method V

When estimates of the parameters in the model (Eq. 1–4) are available, e.g. through maximum likelihood methods, data can be simulated by so-called parametric bootstrapping (Efron and Tibshirani 1993:53–56). One set of simulated time series produces a parametric bootstrap replication of the scatter diagram.

Method VI

Alternatively, we can perform parametric bootstrapping using only the error terms W_{it} , which are supposed to have the same correlation structure as the D_{it} values. The error terms have a distribution independent on α and β , hence only estimates of σ , ρ_∞ , ρ_0 and l (Eq. 1) are required. A bootstrap replicate of the scatter diagram is then calculated from the simulated error terms.

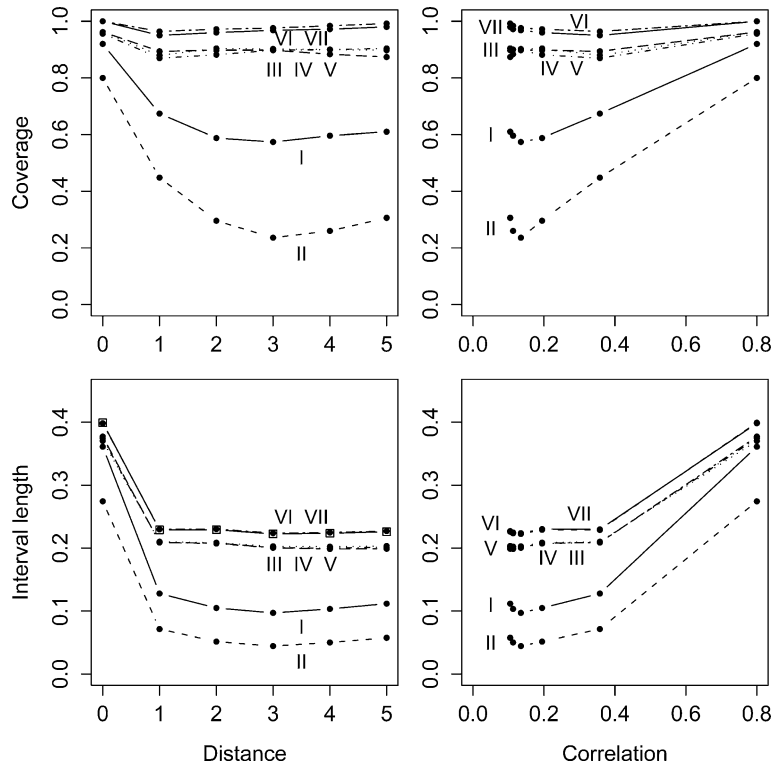
Results

Time series of length $T=20$ for the growth rate $D = \Delta \ln N$ were simulated for $n=30$ locations. The correlogram (Fig. 1) was defined by the parameter values $\rho_0=0.8$, $\rho_\infty=0.1$ and $l=1$, and the environmental variance σ^2 was equal to 0.01, which is a typical order of environmental variance for many species (Lande et al. 2003:18–24). The locations were selected at random from a uniform distribution on a square with side length $5l=5$ and then fixated. The initial density values $\ln N_{10}, \dots, \ln N_{n0}$, generated from a normal distribution with mean α/β and variance $\sigma^2 l \{1 - (1-\beta)^2\}$, were also fixated for each choice of α and β .

For each bootstrap replication of the scatter diagram the method of least squares was used to estimate the correlogram, assuming that the mathematical function of the correlogram was known. Based on $B=1000$ bootstrap replications of the estimated correlogram, nominal 95% bootstrap confidence intervals for $\rho(z)$ (Eq. 6) were calculated for the distances $z=0, 1, \dots, 5$. In order to examine the sample properties of these intervals, the procedure was repeated 500 times, simulating a new set of time series for each repetition, giving the coverage, i.e. the relative frequency of intervals which covered $\rho(z)$, and the mean length of the intervals.

Figure 2 and 3 give the results for time series with different density regulation. The estimated coverage and mean length of the bootstrap confidence intervals are plotted as a function of spatial distance and spatial correlation. Resampling of locations (methods I and II) give confidence intervals with coverage far below the nominal level of 95%, for method II as low as 30%. Resampling of timepoints (methods III, IV and V) give intervals with level around 90% when we have weak density regulation (Fig. 2) whilst the coverage using

Fig. 2. Coverage, defined as the relative frequency of confidence intervals that cover $\rho(z)$, and mean length of nominal 95% confidence intervals for $\rho(z)$ under weak density regulation in relation to distance z and spatial correlation $\rho(z)$ for different estimation methods I–VII (Table 1). The parameters are $\rho_0=0.8$, $\rho_\infty=0.1$, $l=1$, $\alpha=0.2$, $\beta=0.03$ and $\sigma^2=0.01$ (Eq. 1–4). Initial values for the density $\ln N$ were generated from a normal distribution with mean 6.67 and variance 0.17.



method III decreases to around 80% in case of higher density regulation (Fig. 3). Methods VI and VII (parametric bootstrapping) give confidence intervals with coverage around 97–98%, i.e. in fact over the nominal level of 95%. In general we see that methods giving the highest coverage also give the longest confidence inter-

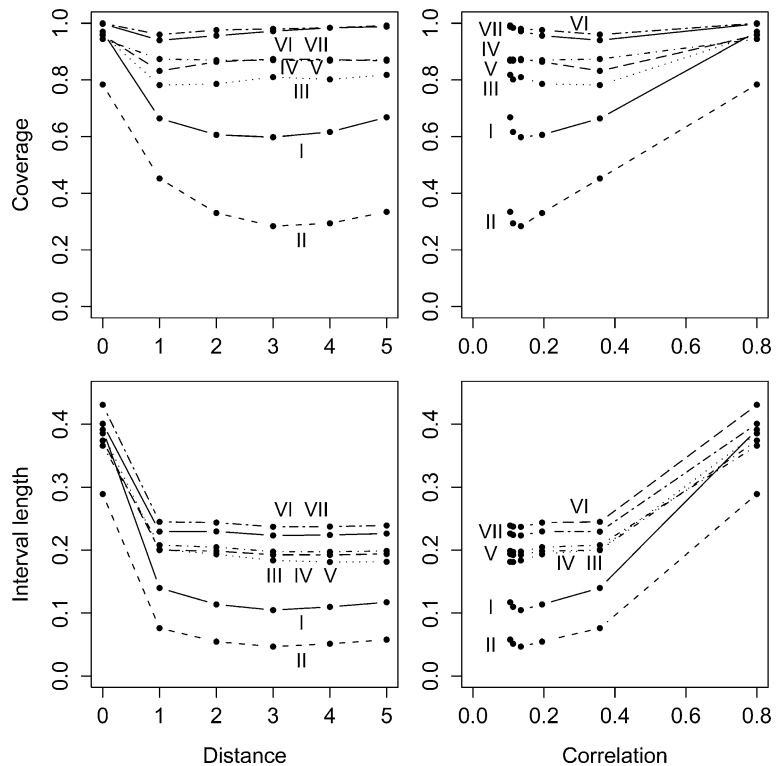


Fig. 3. Coverage, defined as the relative frequency of confidence intervals that cover $\rho(z)$, and mean length of nominal 95% confidence intervals for $\rho(z)$ under strong density regulation in relation to distance z and spatial correlation $\rho(z)$ for different estimation methods I–VII (Table 1). The parameters are $\rho_0=0.8$, $\rho_\infty=0.1$, $l=1$, $\alpha=4$, $\beta=0.6$ and $\sigma^2=0.01$ (Eq. 1–4). Initial values for the density $\ln N$ were generated from a normal distribution with mean 6.67 and variance 0.012.

vals, as should be expected. The coverage is also highest for small distances where the spatial correlation is high.

Discussion

We have seen that different bootstrapping procedures for construction of confidence intervals for spatial correlation in short time series give rather different results for the coverage as well as interval length (Fig. 2, 3). Methods I and II, non-parametric resampling of locations and pairs of locations, both perform extremely bad, as nominal 95% confidence intervals may have coverage as small as 30–40% only, especially for small correlations at large distances. This occurs in strongly as well as weakly density-regulated populations (Fig. 2, 3). Using these methods would give the impression that the spatial correlation function is estimated with a much larger precision than what is actually possible. Resampling of timepoints, methods III, IV and V, perform much better, although the coverage also for these methods is too small (about 90%), except for small distances where the correlation is large. The only method that gives approximately correct coverage is parametric bootstrapping, methods VI and VII. These methods, however, have the disadvantage that the mathematical form of underlying model is assumed to be known, but these results demonstrate how important knowledge about the model is. Rather surprisingly, there is little difference between the results for strongly and weakly density regulated populations (Fig. 2, 3). When density regulation is weak, the pairs of observations (from two different locations) are almost independent through time, which is not the case when the density-regulation is strong. The data will therefore contain more information about the correlations when the density regulation is weak, but it is apparent from Fig. 2 and 3 that, in our example, this effect was rather small. However, it may still affect analyse of an expected (Hanski 1990) relationship between degree of synchrony and local population variability.

Bootstrapping is generally based on replacing the distribution generating the data by an estimated empirical distribution. The set of observations at a given point of time is one observation from a multivariate normal distribution. If the density regulation is weak, we have T approximately independent observations from a multivariate normal distribution. When we resample timepoints (methods III–V), we actually replace the distribution of this multivariate variable by its empirical distribution in agreement with the basic idea of bootstrapping. Methods I and II, however, can not be interpreted as such sampling from an empirical distribution, which may be the reason why it fails so dramatically (Fig. 2, 3). Parametric bootstrapping (methods VI and VII) are resampling from the estimated parametric

distribution, and is also consistent with the general idea of bootstrapping.

Density regulation is an important concept in population dynamics and the problems of detecting it from short time series has been discussed by several authors (Bulmer 1975, Zeng et al. 1998). In particular, if the density regulation is weak, the data will contain little information about the carrying capacity (Lande et al. 2002) so that estimating carrying capacity and detecting density regulation or accurately estimating it will be difficult. This estimation problem in weakly regulated populations, however, has no analogy when it comes to estimating spatial correlations. In this case weak density regulation is an advantage because it makes temporal differences less dependent.

The estimation of spatial autocorrelations, and correct computation of uncertainty in this estimation, is an important part of population dynamics because the autocorrelation itself is related directly to the underlying biological processes. Several studies, (Ranta et al. 1997, Lande et al. 1999, Bjørnstad and Bolker 2000, Kendall et al. 2000, Engen 2001, Engen et al. 2002a, b, 2004) has explored theoretically how migration, spatial autocorrelation in the noise, strength of density-regulation as well as permanent spatial heterogeneity affects spatial autocorrelation of population fluctuations. Engen et al. (2004) showed that the residuals with respect to a stochastic population models also will be affected by migration, but this effect will only be apparent on relatively small distances. Thus, the scaling of the residuals will essentially reveal the spatial scaling of the environmental noise.

References

- Bjørnstad, O. N. and Bolker, B. 2000. Canonical functions for dispersal-induced synchrony. – Proc. R. Soc. Lond. B 267: 1787–1794.
- Bjørnstad, O. N. and Falck, W. 2001. Nonparametric spatial covariance functions: Estimation and testing. – Environ. Ecol. Stat. 8: 53–70.
- Bjørnstad, O. N., Ims, R. A. and Lambin, X. 1999a. Spatial population dynamics: analyzing patterns and processes of population synchrony. – Trends Ecol. Evol. 14: 427–432.
- Bjørnstad, O. N., Stenseth, N. C. and Saitoh, T. 1999b. Synchrony and scaling in dynamics of voles and mice in northern Japan. – Ecology 80: 622–637.
- Bulmer, M. G. 1975. Statistical analysis of density dependence. – Biometrics 31: 901–911.
- Buonaccorsi, J. P., Elkinton, J. S., Evans, S. R. et al. 2001. Measuring and testing for spatial synchrony. – Ecology 82: 1668–1679.
- Cattadori, I. M., Hudson, P. J., Merler, S. et al. 1999. Synchrony, scale and temporal dynamics of rock partridge (*Alectoris graeca saxatilis*) populations in the Dolomites. – J. Anim. Ecol. 68: 540–549.
- Cattadori, I. M., Merler, S. et al. 2000. Searching for mechanisms of synchrony in spatially structured gamebird populations. – J. Anim. Ecol. 69: 620–638.
- Chilès, J.-P. and Delfiner, P. 1999. Geostatistics. Modeling spatial uncertainty. – Wiley.

- Cressie, N. A. C. 1993. Statistics for spatial data. Revised ed. – Wiley.
- Dennis, B., Kemp, W. P. and Taper, M. L. 1998. Joint density dependence. – *Ecology* 79: 426–441.
- Efron, B. and Tibshirani, R. J. 1993. An introduction to the bootstrap. – Chapman and Hall, London.
- Engen, S. 2001. A dynamic and spatial model with migration generating the log-Gaussian field of population densities. – *Math. Biosci.* 173: 85–102.
- Engen, S., Lande, R. and Sæther, B.-E. 2002a. Migration and spatiotemporal variation in population dynamics in heterogeneous environment. – *Ecology* 83: 570–579.
- Engen, S., Lande, R. and Sæther, B.-E. 2002b. The spatial scale of population fluctuations and quasi-extinction risk. – *Am. Nat.* 160: 439–451.
- Engen, S., Lande, R., Sæther, B.-E. et al. 2004. Estimating the pattern of synchrony in fluctuating populations, *J. Anim. Ecol.* in press.
- Fisher, R. A. 1915. Frequency distribution of the values of the correlation coefficient in samples of an indefinitely large population. – *Biometrika* 10: 507–521.
- Fisher, R. A. 1921. On the ‘probable error’ of a coefficient of correlation deduced from a small sample. – *Metron* 1: 3–32.
- Hanski, I. 1990. Density dependence, regulation and variability in animal populations. – *Philos. Trans. R. Soc. B* 330: 141–150.
- Hanski, I. and Woiwood, I. P. 1993. Spatial synchrony in the dynamics of moth and aphid populations. – *J. Anim. Ecol.* 62: 656–668.
- Haydon, D. T., Stenseth, N. C., Boyce, M. C. et al. 2001. Phase coupling and synchrony in the spatiotemporal dynamics of muskrat and mink populations across Canada. – *Proc. Natl Acad. Sci. USA* 98: 13149–13154.
- Johnsen, R. A. and Wichern, D. W. 1988. Applied multivariate statistical analysis. – Prentice-Hall.
- Kendall, B. E., Bjørnstad, O. N., Bascompte, J. et al. 2000. Dispersal, environmental correlation, and spatial synchrony in population dynamics. – *Am. Nat.* 155: 628–636.
- Koenig, W. D. 1999. Spatial autocorrelation of ecological phenomena. – *Trends Ecol. Evol.* 14: 22–26.
- Koenig, W. D. 2002. Global patterns of environmental synchrony and the Moran effect. – *Ecography* 25: 283–288.
- Lahiri, S. N., Kaiser, M. S., Cressie, N. et al. 1999. Prediction of spatial cumulative distribution functions using subsampling. – *J. Am. Stat. Assoc.* 94: 86–99.
- Lande, R., Engen, S. and Sæther, B.-E. 1999. Spatial scale of population synchrony: environmental correlation versus dispersal and density regulation. – *Am. Nat.* 154: 271–281.
- Lande, R., Sæther, B.-E., Engen, S. et al. 2002. Estimating density dependence from population time series using demographic theory and life-history data. – *Am. Nat.* 159: 321–332.
- Lande, R., Engen, S. and Sæther, B.-E. 2003. Stochastic population dynamics in ecology and conservation. – Oxford Univ. Press.
- Lindström, J., Ranta, E. and Lindén, H. 1996. Large-scale synchrony in the dynamics of capercaillie, black grouse and hazel grouse populations in Finland. – *Oikos* 76: 221–227.
- Matheron, G. 1962. *Traite de geostatistique appliquee*, tome I. Mem. Bureau Recherches Geologiques Minières, No. 14. Editions Technip. – Paris.
- Moran, P. A. P. 1953. The statistical analysis of the Canadian lynx cycle. II. Synchronization and meteorology. – *Aust. J. Zool.* 1: 291–298.
- Myers, J. H. 1998. Synchrony in outbreaks of forest Lepidoptera: a possible example of the Moran effect. – *Ecology* 79: 1111–1117.
- Myers, R. A., Mertz, G. and Bridson, J. 1997. Spatial scales of interannual recruitment variations of marine, anadromous, and freshwater fish. – *Can. J. Fish. Aquat. Sci.* 54: 1400–1407.
- Paradis, E., Baillie, S. R., Sutherland, W. J. and Gregory, R. D. 1999. Dispersal and spatial scale affect synchrony in spatial population dynamics. – *Ecol. Lett.* 2: 114–120.
- Paradis, E., Baillie, S. R., Sutherland, W. J. et al. 2000. Spatial synchrony in populations of birds: effects of habitat, population trend, and spatial scale. – *Ecology* 81: 2112–2125.
- Peltonen, M., Liebhold, A. M., Bjørnstad, O. N. et al. 2002. Spatial synchrony in forest insect outbreaks: roles of regional stochasticity and dispersal. – *Ecology* 83: 3120–3129.
- Ranta, E., Lindström, J. and Lindén, H. 1995. Synchrony in tetraonid population-dynamics. – *J. Anim. Ecol.* 64: 767–776.
- Ranta, E., Kaitala, V. and Lundberg, P. 1997. The spatial dimension in population fluctuations. – *Science* 278: 1621–1623.
- Ranta, E., Kaitala, V. and Lindström, J. 1998. Spatial dynamics of populations. – In: Bascompte, J. and Solé, R. V. (eds), *Modeling spatiotemporal dynamics in ecology*. Springer-Verlag, pp. 47–62.
- Roughgarden, J. 1975. A simple model for population-dynamics in stochastic environments. – *Am. Nat.* 109: 713–736.
- Royama, T. 1992. Analytical population dynamics. – Chapman and Hall.
- Sutcliffe, O. L., Thomas, D. C. and Moss, D. 1996. Spatial synchrony and asynchrony in butterfly dynamics. – *J. Anim. Ecol.* 65: 85–95.
- Tobin, P. C. and Bjørnstad, O. N. 2003. Spatial dynamics and cross-correlation in a transient predator–prey system. – *J. Anim. Ecol.* 72: 460–467.
- Viljugrein, H., Lingjærde, O. C., Stenseth, N. C. et al. 2001. Spatio-temporal patterns of mink and muskrat in Canada during a quarter century. – *J. Anim. Ecol.* 70: 671–682.
- Williams, C. K., Ives, A. R. and Applegate, R. D. 2003. Population dynamics across geographical ranges: time-series analyses of three small game species. – *Ecology* 84: 2654–2667.
- Williams, D. W. and Liebhold, A. M. 2000. Spatial synchrony of spruce budworm outbreaks in eastern North America. – *Ecology* 81: 2753–2766.
- Winkler, G. 1995. Image analysis, random fields and dynamic Monte Carlo methods. – Springer Verlag.
- Zeng, Z., Nowierski, R. M., Taper, M. L. et al. 1998. Complex population dynamics in the real world: Modeling the influence of time-varying parameters and time lags. – *Ecology* 79: 2193–2209.
- Zhu, J. and Morgan, G. D. 2004. Comparison of spatial variables over subregions using a block bootstrap. – *J. Agr. Biol. Environ. Stat.* 9: 91–104.

Appendix 1.

Estimation of spatial covariance in the case of one observation per location

When there is only one observation x_i per location, $i = 1, \dots, n$, the spatial covariance between locations i and j is sometimes estimated by

$$(x_i - \bar{x})(x_j - \bar{x}) \quad (7)$$

where \bar{x} is the sample mean of x_1, \dots, x_n (Bjørnstad et al. 1999b, Bjørnstad and Falck 2001, Tobin and Bjørnstad 2003). The motivation for this is probably the standard definition of covariance

$$\text{cov}(X_i, X_j) = E\{(X_i - \mu)(X_j - \mu)\}$$

when we have a common mean μ for all locations.

However, the findings using (7) may be partly a statistical artifact. This is seen from the equality

$$\left\{ \sum_{i=1}^n (x_i - \bar{x}) \right\}^2 = \sum_{i=1}^n (x_i - \bar{x})^2 + 2 \sum_{i < j} (x_i - \bar{x})(x_j - \bar{x}) = 0$$

We have $\sum_{i=1}^n (x_i - \bar{x})^2 \geq 0$ and consequently $\sum_{i < j} (x_i - \bar{x})(x_j - \bar{x}) \leq 0$, that is, some estimated covariances are forced to be negative, which is a problem in a situation when all the true covariances are positive.

Define a new variable $Y_i = X_i + W$, $i = 1, \dots, n$, where W is an exogenous factor having the same influence on all locations. If W is large compared to the X_i s, the spatial covariance between all locations should be positive. But

$$(y_i - \bar{y})(y_j - \bar{y}) = (x_i - \bar{x})(x_j - \bar{x})$$

and consequently some covariances are still forced to be negative. That is, the effect of W cannot be discovered, and a long distance correlation $\rho_\infty \neq 0$ cannot be estimated. Consequently we expect the estimator to be most biased when the spatial covariance or correlation is large.

The bias of the estimator in (7) is defined as the difference between the expected value of the estimator and the true covariance, that is

$$E\{(X_i - \bar{X})(X_j - \bar{X})\} - \text{cov}(X_i, X_j)$$

Calculations show that this bias turns out to be

$$-\frac{1}{n} \left[\sum_{k=1}^n \{\text{cov}(X_i, X_k) + \text{cov}(X_j, X_k)\} - \frac{2}{n} \sum_{k < l} \text{cov}(X_k, X_l) - \text{var}(X_i) \right]$$

which is most negative when the covariances $\text{cov}(X_i, X_k)$ are large, as expected. The estimated covariance function in relation to distance is plotted in Fig. 4.

Serial correlation in growth rates

In a time series $\{\ln N_t\}_{t=1}^T$ the autocovariance function C is defined by $C(s) = \text{cov}(\ln N_t, \ln N_{t+s})$ and the autocorrelation function ρ by $\rho(s) = C(s)/C(0)$. Define the time series

$$\ln N_t = \alpha + (1 - \beta)\ln N_{t-1} + W_t, \quad t = 1, \dots, T$$

where W_1, \dots, W_t are independent equally distributed with mean zero. We have

$$C(s) = (1 - \beta)^s \text{var}(\ln N_t) = (1 - \beta)^s C(0)$$

and $\rho(s) = (1 - \beta)^s$. Now, define the growth rate $D_t =$

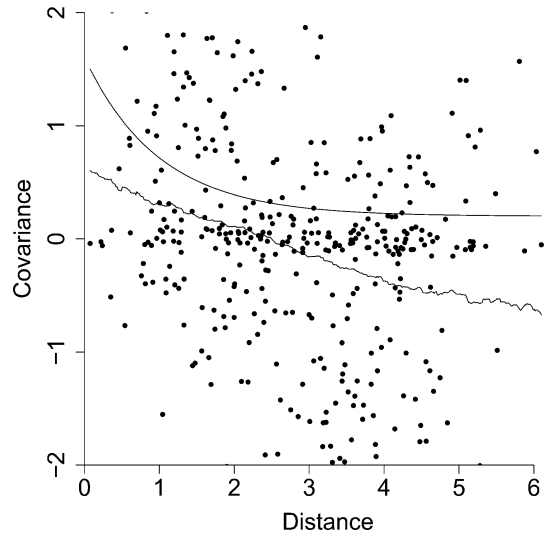


Fig. 4. Scatter diagram of distance and estimated covariance between locations (Eq. 7). The data were generated from locations with spatial covariance decreasing from 1.6 for small distances to 0.2 for long distances (upper line). The estimated covariance function (lower line) is calculated from the scatter diagram using a nonparametric method. We have the sum of estimated covariances $\sum_{i < j} (x_i - \bar{x})(x_j - \bar{x}) = -24.0$.

$\ln N_t - \ln N_{t-1}$. Then

$$\begin{aligned} \text{cov}(D_t, D_{t+s}) &= \text{cov}(\ln N_t - \ln N_{t-1}, \ln N_{t+s} - \ln N_{t+s-1}) \\ &= 2C(s) - C(s+1) - C(s-1) \end{aligned}$$

Using the equality $C(s) = C(-s)$,

$$\text{cov}(D_t, D_t) = 2C(0) - 2C(1).$$

Hence, the autocorrelation between D_t and D_{t+s} is given by

$$\begin{aligned} &\frac{2C(s) - C(s+1) - C(s-1)}{2C(0) - 2C(1)} \\ &= \frac{2\rho(s) - \rho(s+1) - \rho(s-1)}{2 - 2\rho(1)} \\ &= \frac{2(1 - \beta)^s - (1 - \beta)^{s+1} - (1 - \beta)^{s-1}}{2 - 2(1 - \beta)} \\ &= -\frac{\beta}{2}(1 - \beta)^{s-1}, \quad s^3 \geq 1 \end{aligned}$$

We see that the autocorrelation is zero when there is no density dependence ($\beta = 0$). For maximum density dependence ($\beta = 1$) we have autocorrelation -0.5 when $s = 1$ and zero for $s \geq 2$.